Earth Surface Processes and Landforms
Earth Surf. Process. Landforms **31**, 123–132 (2006)
Published online in Wiley InterScience (www.interscience.wiley.com). **DOI:** 10.1002/esp.1315

Letter to ESEX

A cellular model of river meandering

Tom. J. Coulthard[1]* and Marco. J. Van De Wiel[2]
[1] *Department of Geography, University of Hull, Hull, HU6 7RX, UK*
[2] *Department of Geography, University of Western Ontario, London, Ontario, N6A 5C2, Canada*

**Correspondence to:*
T. J. Coulthard, Department of Geography, University of Hull, Cottingham Road, Hull, HU6 7RX.
E-mail: T.Coulthard@hull.ac.uk

Received 12 July 2005;
Revised 20 October 2005;
Accepted 25 October 2005

Abstract

River meandering has been successfully modelled using vector based methods, but these can not simulate multiple or braided channels. Conversely, cellular braided river models fail to replicate meandering. This paper describes a new method to simulate river meandering within a cellular model (CAESAR). A novel technique for determining bend radius of curvature on a cell by cell basis is described, that importantly allows regional information on bend curvature to be transferred to local points. This local curvature is then used to drive meandering and lateral erosion through two methods. Key difficulties are identified, including the deposition of material on point bars and cut off development, but the method illustrates how meandering can be integrated within a cellular framework. This demonstrates the potential to produce a single model that can incorporate both meandering and braiding. Copyright © 2006 John Wiley & Sons, Ltd.

Keywords: meandering, braiding, cellular model

Introduction and Rationale

The past few decades have seen significant improvements in our understanding of the processes that lead to river meandering and braiding. Although fundamental questions as to the causes of the variety in river patterns remain, it is clear that there is a continuum of river patterns between straight, meandering and braiding. Yet there is a clear dichotomy in numerical models for these various channels types. Straight and meandering rivers are usually simulated using vector-based models (e.g. Howard, 1992, 1996; Sun *et al*., 1996, 2001b), which elegantly capture the dynamics of single-thread channels, but which cannot simulate multi-threaded channels. Conversely, braided channels are effectively simulated using cellular-based models (e.g. Murray and Paola, 1994; Thomas and Nicholas, 2002), which use simple local rules to replicate the dynamics of the system, yet fail to replicate the lateral dynamics of meandering channels. This dichotomy unfortunately hinders the development of generic fluvial landscape evolution models and hampers the furthering of theoretical understanding of fluvial systems. Indeed, unifying meandering and braiding in one cellular modelling scheme has been proclaimed as the 'holy grail' of planform modelling (Paola, 2000). In this paper we present a possible solution to cellular modelling of river meandering and discuss its potential and implications.

Meandering Models

The causes and impacts of river meandering have captivated researchers for years. Although debate still surrounds the precise causes of river meandering, it is now accepted that secondary circulation, i.e. flow not parallel to the main channel direction, can preferentially erode one river bank and deposit material at the toe of the other. Thus a positive feedback is established, whereby increased asymmetry of the flow increases secondary circulation, thus promoting further lateral erosion along the outside bank.

Over the last 30 years, several numerical models have been developed to investigate river meandering. Initially, these were based upon random walks (Ferguson, 1976), but these were superseded by theoretical approaches based on

a linearization of the St. Venant flow equations (Ikeda *et al*., 1981; Blondeaux and Seminara, 1985; Johannesson and Parker, 1989; Sun *et al*., 2001a). Referred to herein as IPS models, after the original publication (Ikeda *et al*., 1981), these models relate lateral bank migration, ζ, to near-bank flow velocity, u_{nb}, which in turn is a function of channel curvature, R_c:

$$\zeta = E_0 u_{nb} \tag{1}$$

$$u_{nb} = f(R_c, u_0, h_0, b, C_f) \tag{2}$$

where E_0 denotes a bank erosion coefficient (Ikeda *et al*., 1981; Hasegawa, 1989), b is a fixed channel width, and u_0, h_0 and C_f respectively denote cross-sectional averages of flow velocity, flow depth and friction factor. Equation 1 has also been obtained from empirical data (Howard and Knutson, 1984). Several models have been developed using this approach (Howard and Knutson, 1984; Howard, 1992, 1996; Sun *et al*., 1996, 2001b), in which a fixed-width channel is represented by its centre-line, split by nodes into links. The radius of curvature can be calculated between these links and is used to drive the lateral movement of the channel by shifting the line or links laterally according to Equations 1 and 2. Therefore, using the radius of curvature derived from the planform, this simulates the feedback described in the first paragraph, whereby increased lateral erosion reduces the radius of curvature (tightening the bend) which further increases lateral erosion. Where two lines touch, a cut-off can form, allowing the development of ox-bow lakes. More recent approaches (Lancaster and Bras, 2002) have used the concept of topographic steering. Instead of relating lateral erosion to planform curvature, they use the cross-stream angle of the river bed or the cross-channel slope to drive lateral erosion. Similar to the IPS approaches using radius of curvature, a steeper cross-bed gradient will produce more lateral erosion, thus driving meander development.

These vector-based models have produced some qualitatively and quantitatively realistic meandering channel patterns, and demonstrated how meandering can be controlled by planform curvature or bed topography, as well as how factors such as valley floor width and cut-off rate influence floodplain and meander-belt development (Howard and Knutson, 1984; Howard, 1992, 1996; Sun *et al*., 1996, 2001b). However, there are some important limitations with these schemes.

1. All these models simulate meandering channels as being single-threaded, whereas rivers may have islands, or fluctuate between being braided and meandering.
2. They all assume a fixed channel width and there is no in-channel topography (e.g. medial bars or pools and riffles).
3. There is no continuity of sediment, as they (largely) assume that material is deposited on the inside edge of the bend at the same rate as it is eroded along the outside bank. This is rarely the case in reality, as the geometry of channels means more sediment is eroded at the outside edge than can be deposited on the inside (see Lauer and Parker, 2005).

Cellular Braided River Models

Cellular automaton (CA) models have shown great promise in simulating braided streams (Murray and Paola, 1994; Thomas and Nicholas, 2002) and landscape evolution (Coulthard and Macklin, 2003; Coulthard *et al*., 2000, 2002), but without the capability to meander. This is largely because they simplify the complex equations used to calculate flow, partly to find a parsimonious explanation, but also to reduce computation time, which in turn allows sediment transport and morphological change to be modelled. By using simple empirical flow equations, such as Manning's or Chezy, the terms for momentum and for describing secondary circulation are lost. Furthermore, the cellular discretization, where each cell only has knowledge of itself and its immediate neighbours, makes it difficult to determine whether a cell is (a) part of a bank, (b) next to a bank, (c) part of a bend, (d) part of an inside or outside bend, and (e) the momentum and direction of water entering a cell.

This has so far prevented meandering from being incorporated in such CA models, as meandering is determined by 'regional' rules (channel plan-form and circulation patterns) whereas cellular braided models only have knowledge of 'local' flow parameters (at a point depth and velocity). Therefore, the capability to provide CA models with such regional data could allow a unified cellular braided–meandering model to be developed.

Here, we propose a solution, by presenting a methodology to simulate lateral erosion and river meandering within a cellular model. Firstly, we present a novel methodology to determine the radius of curvature on a cell-by-cell basis. Secondly, we show how we use this to simulate lateral channel movement and meandering within a cellular landscape evolution model.

Method

Determining radius of curvature

The algorithm is straightforward with four steps. It operates over a matrix or grid where water depths for a channel pattern have been previously determined (for example Figure 1) and assumes that this grid can simply be divided into wet and dry cells.

1. Firstly, a pass is made over the grid identifying which cells are 'edge' cells. These are defined as 'dry' cells with a wet neighbour in the north, south, east or west direction (where x and y are Cartesian co-ordinates: $x-1$, $x+1$, $y-1$, $y+1$). Diagonal edge cells are not included (Figure 1).
2. Secondly, a nine-cell filter (Figure 2a, b and c) is passed over grid. Where there is an edge cell at the centre of the filter, the number of dry and wet cells is summed including diagonals. Importantly, any other edge cells within the filter are excluded from this calculation.
3. The number of wet cells is then subtracted from the number of dry and this value is assigned to the edge cell at the centre of the filter. This value represents a local expression of radius of curvature (balance of wet and dry cells), while its sign identifies inside (negative) and outside (positive) banks. However, due to the discretization into a cellular grid, a meander bend can contain elements of both inside and outside banks. As such, the balance of wet and dry cells provides a very 'rough' measure of curvature (see Figures 1 and 2).
4. Lastly, to reduce the roughness of the curvature calculation, a smoothing filter is repeatedly passed over the edge cells, averaging the curvature between adjacent edge cells (including any diagonal edge neighbours). Therefore, the value assigned to an edge cell represents a moving average of the balance of wet and dry cells either side of an edge cell. The number of smoothing passes was determined experimentally and is described later.

This generates a cellular automaton curvature term (R_{ca}) for each of the edge cells, (as shown in Figure 5a) for a section of the river Teifi near Lampeter, mid-Wales, UK.

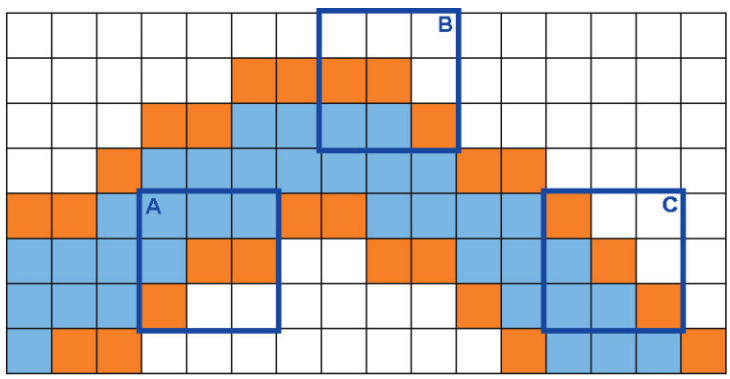

Figure 1. A section of river channel, discretized into grid cells. Blue cells correspond to wet cells, white are dry and red are edge cells. This figure is available in colour online at www.interscience.wiley.com/journal/espl

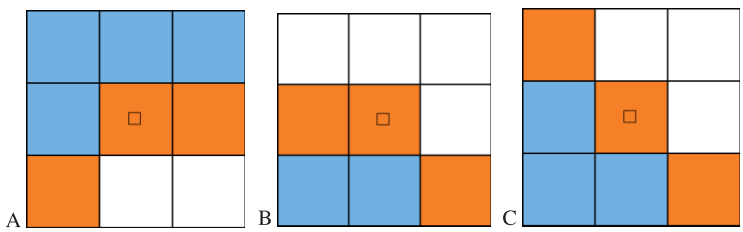

Figure 2. Sections A, B and C from Figure 1. These represent inside, outside and straight sections of channel respectively. This figure is available in colour online at www.interscience.wiley.com/journal/espl

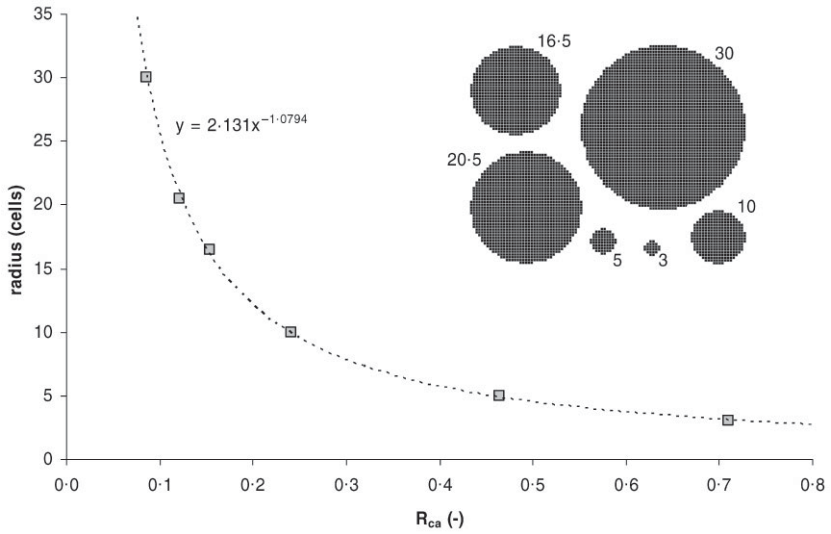

Figure 3. Relation between the cellular automaton curvature term (R_{ca}) and radius (expressed as number of grid cells) for a range of different size circles (inset)

Table I. Comparison of calculated to actual radii of curvature at different grid resolutions.

Resolution (*Res*, cell size, m)	Actual radius (*R*, no. cells)	CA curvature algorithm result (R_{ca}, dimensionless)	Calculated radius, $R_{cal} = 2{\cdot}131\ R_{ca}^{-1{\cdot}0794}$ (R_{cal}, no. cells)	Actual radius, $R \times Res$ (m)	Calculated radius, $R_{cal} \times Res$ (m)
3	30	0·085	30·441	3 × 30 = 90	91·324
9	10	0·240	9·925	9 × 10 = 90	89·327
30	3	0·710	3·085	30 × 3 = 90	92·564

A series of numerical experiments was carried out in order to relate the R_{ca} term to the actual radius of curvature. Within a spreadsheet, several circles of varying radii were discretized into a cellular grid, with areas inside the circles being 'wet' and those outside 'dry'. Steps 1–4 (above) were then applied to the circles. Figure 3 describes the results, showing that there was an excellent relationship between the calculated R_{ca} and the actual radius of curvature in cells ($R = 2{\cdot}131\ R_{ca}^{-0{\cdot}10794}$). Furthermore, the radius of curvature in cells has only to be multiplied by the cell size in order to produce the actual radius of curvature, indicating the method can be easily applied over a range of grid scales. This is shown in Table I where very similar radii of curvature are calculated for a three-cell circle with 30 m cells, a nine-cell circle with 10 m cells and a 30-cell circle with 3 m cells.

The data plotted in Figure 3 were produced after five passes of the smoothing filter. We carried out sensitivity analyses to determine the optimum number of passes required. Figure 4a indicates how the curvature term drops then rapidly stabilizes for all circles measured. Figure 4b shows how the standard deviation of the calculated curvature term drops. We chose five iterations as the optimum point. However, when applied to genuine meander bends, there may be sensitivity to the length of the number of filter passes.

One further benefit of this algorithm is that it provides curvature terms for both the outside of the bend (a positive number) and for the inside (negative number) as shown by the shading in Figure 5a.

Generating lateral erosion and deposition

Within a cellular model, calculating lateral erosion from the R_{ca} term is straightforward. However, channel migration and thus meandering also requires deposition on the inside bend and is significantly more complex. This section briefly discusses two methods to simulate lateral erosion and deposition. Unlike the previous section, these methods are not validated and are only qualitatively tested. Therefore, we propose to use them as evidence that the R_{ca} term can be used to drive lateral erosion, and to position them as a starting point for further development. Both schemes and the

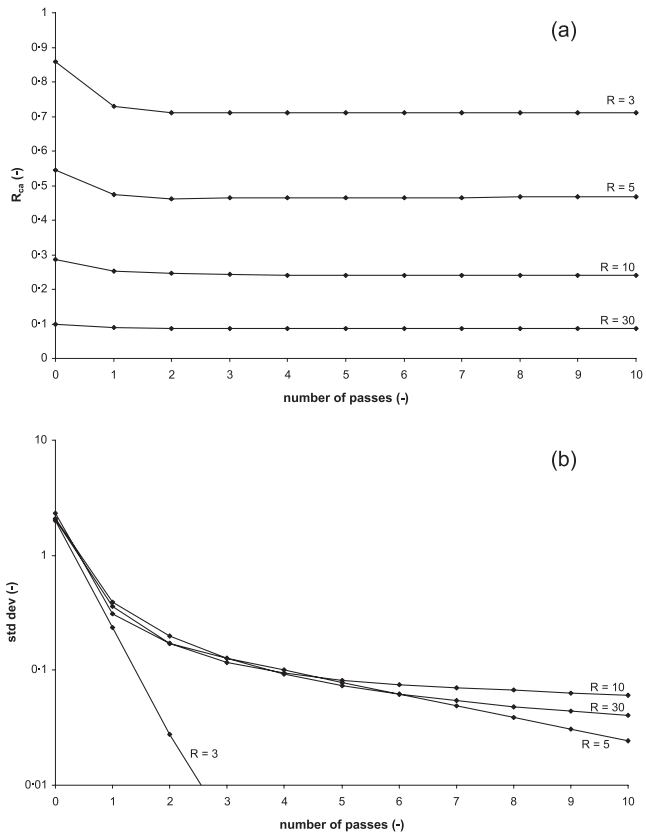

Figure 4. Influence of number of passes of the smoothing filter on (a) the value of R_{ca} for different sized circles, and (b) the standard deviation of R_{ca}

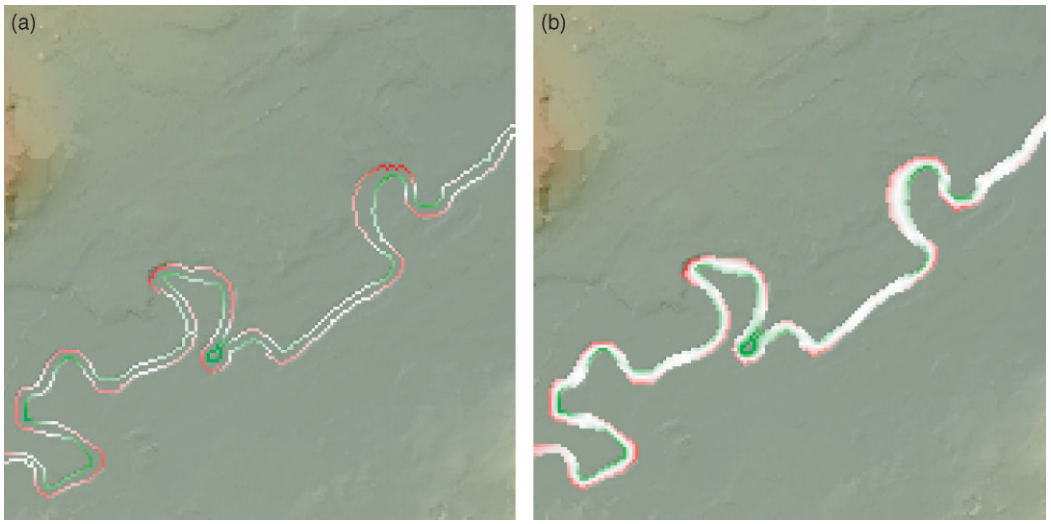

Figure 5. Application of algorithms to a 10 m LiDAR-generated DEM of a reach of the River Teifi, near Lampeter, UK. Flow is from left to right. (a) Identification of inside (green) and outside (red) bends, as well as the curvature term, R_{ca}. (b) Cross-stream curvature gradient. This figure is available in colour online at www.interscience.wiley.com/journal/espl

R_{ca} algorithm are imbedded within the cellular landscape evolution model CAESAR (Coulthard and Macklin, 2003;Coulthard *et al*., 2000, 2002), although they could easily be integrated within any other cellular model.

Similar to the IPS approach (Equations 1 and 2), we relate lateral bank erosion, ζ, to flow depth, velocity and the curvature term:

$$\zeta = E_{ca} R_{ca} u_{nb} h_{nb} \tag{3}$$

where E_{ca} is a bank erosion coefficient and h_{nb} denotes near-bank flow depth. Within previous vector-based lateral models, this lateral movement has then simply been used to displace the channel position. Here, a finite volume of sediment is removed from the elevations of the cells on the outer bank. In order to maintain mass balance this has to be deposited within the channel, which can be achieved by depositing eroded material in the cell adjacent to the bank. Over a period of time, the elevation of the bank cell will decline until it is low enough to become inundated and thus the next cell will become the bank cell. This process will simulate bank retreat, but poses two large problems for cellular models. Firstly, it leads to an accumulation of sediment at the cell adjacent to the bank which has to be redistributed. However, in cellular models such as CAESAR (Coulthard and Macklin, 2003; Coulthard *et al*., 2000, 2002), this redistribution will occur as a result of the usual fluvial erosion processes operating within the model. Secondly, if the process of bank retreat continues, the channel will continue to widen indefinitely. Whilst much previous work has focused on bank erosion, a key part of the formation and development of meanders is the deposition on the inside of the bend, for example through the aggradation or accretion on a point bar. The vector-based models, by moving the channel position laterally and maintaining channel width, implicitly assume that the amount of deposition on the inside edge of a bend roughly equals the amount of erosion on the outer bank. In a cellular model, however, deposition along the inside bank must follow from the model automaton rules. Ideally, the model should not need to be 'told' where to deposit sediment in order to develop the inside of a bend. Rather, it should be preferentially deposited there due to the hydraulic conditions within the channel. Unfortunately, in most cellular models sediment is routed according to local slopes (in CAESAR bed slope) and there is no representation of secondary circulation, so it is very hard to route or push sediment onto point bars.

In light of these issues, we demonstrate two different approaches to simulating meander development, of varying effectiveness. Here, both methods were applied, using the CAESAR model, to a 1·8 by 1·8 km 10 m resolution LiDAR-derived DEM of a section of the River Teifi near Lampeter, UK. In both simulations lateral erosion process rates were not calibrated, so the time steps are abstract.

In the first method, channel movement is modelled by imitating how the IPS-type models treat erosion and deposition. Sediment is eroded from the outside river bank according to Equation 3 and is added to cells adjacent to the inside bank using the same formula. We assume that eroded material is swept away and lost from the system, and likewise that deposited material 'appears' on inside bends. This produces the lateral erosion patterns shown in Figure 6. These show the extension of all the meander bends, with tighter bends exhibiting more erosion. These also show a tendency to generate wide channels which illustrates the difficulty in simulating inside-bend deposition with this method.

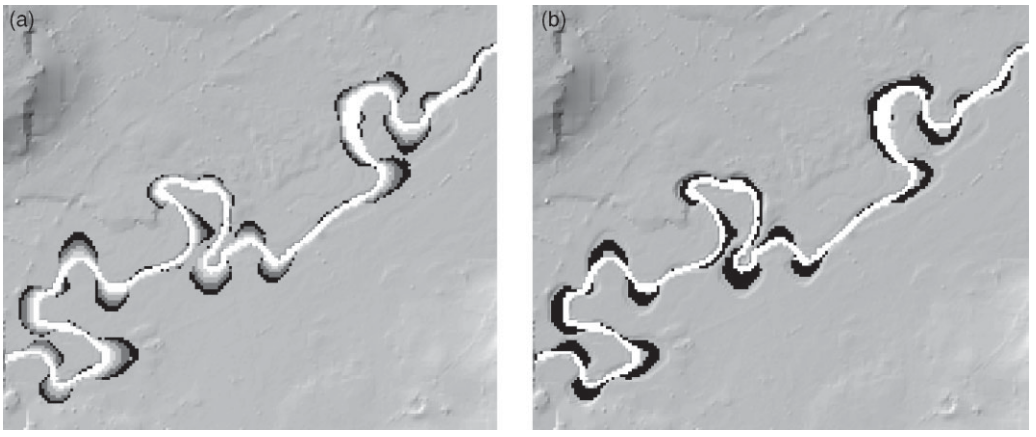

Figure 6. Meander development using method 1. (a) Meander growth; the different shades correspond to five different time slices from the model. (b) Initial and final channel positions

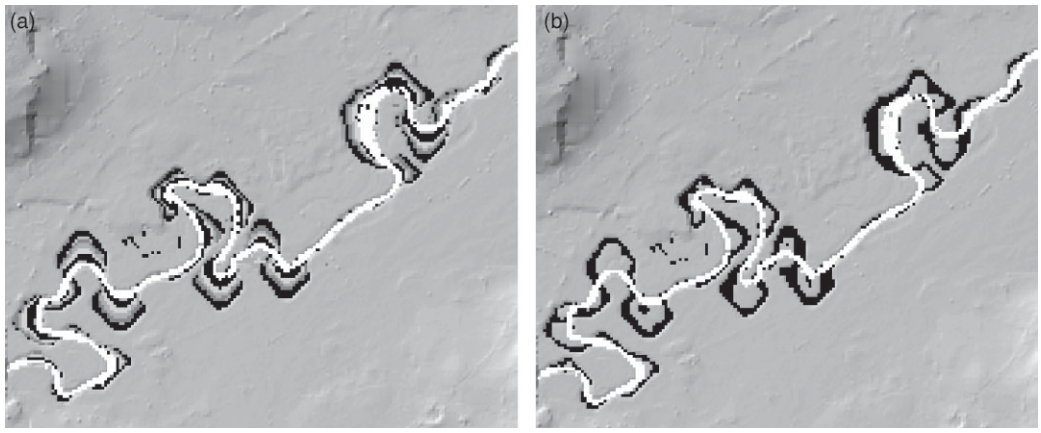

Figure 7. Meander development using method 2. (a) Meander growth; the different shades correspond to five different time slices from the model. (b) Initial and final channel positions

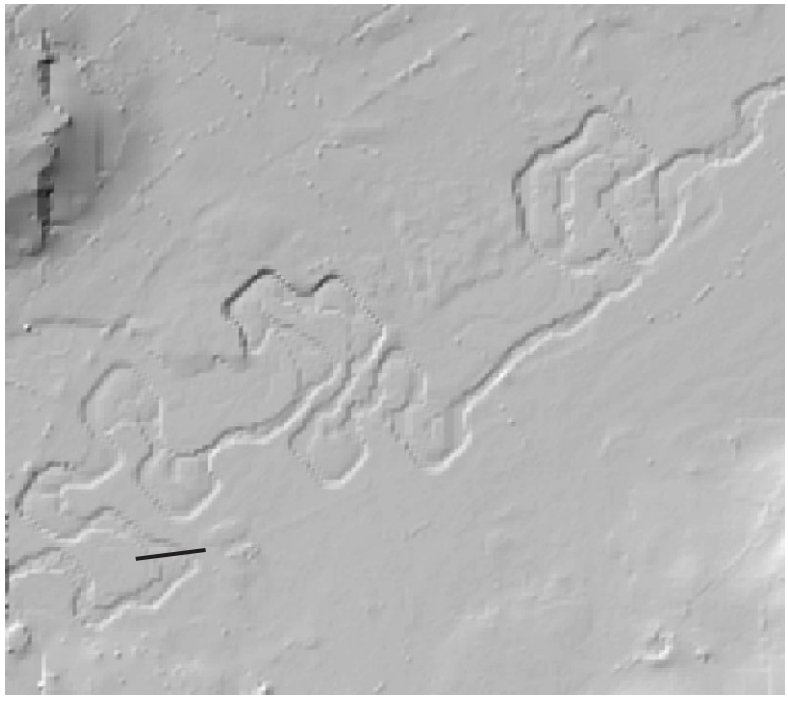

Figure 8. Topography after the simulation using method 2. The line indicates the cross section in Figure 9.

In the second method, erosion of the outside bank is also carried out according to Equation 3. However, the positive (outside) and negative (inside) R_{ca} values are used to determine a cross-stream gradient of curvature. This is carried out by applying an averaging filter across all wet cells to smooth the values across the channel. Results are shown in Figure 5b. This cross-stream gradient of curvature is then used to calculate a lateral sediment flux, ψ_n:

$$\psi_n = a(R_{ca,n} - R_{ca,n-1})h_n \tag{4}$$

where n and $n-1$ respectively denote the donor cell and the receiving cell, a is a coefficient and h is flow depth. Results from this method are presented in Figures 7 and 8. This also generates lateral erosion and meander

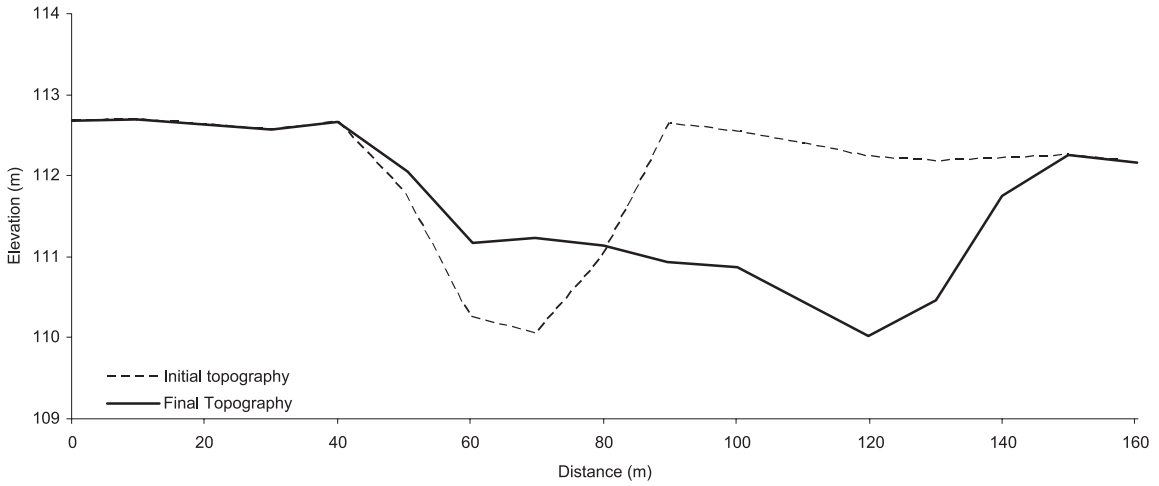

Figure 9. Cross-section from Figure 8 showing initial and final simulated channel cross-sections

migration similar to method 1, but with key differences. The cross-stream movement of sediment creates a narrower, better-defined channel, and also forms point bars on the inside edge of meander bends and a meandering thalweg within the channel. These can be seen on the topography (Figure 8), where the migration of bends has left several large point bars and a switching thalweg between meanders. Figure 9 illustrates a cross-section from Figure 8, showing how this section has changed during the course of the simulation. Interestingly, the northern section of valley floor is restricted by a high terrace, and this has slowed meander migration compared to rates in other parts of the reach. However, the meander bends fail to cut-off where two outside bends intersect (though chutes are evident across point bars) leading to an over-sinuous channel pattern. This is due to the summing of wet and dry edge cells leading to erroneous classification of outside bends just before cut-offs occur. Methods are being prepared to solve this issue. There is also a tendency for bends to migrate faster in the main E–W and N–S directions. This may be a facet of using a regular grid, and may be solved by compensating for the different distances to diagonal neighbours.

Discussion

Both methods are successful in demonstrating how lateral erosion can be simulated in a CA framework. The calculation of the R_{ca} term is robust, and although the lateral erosion algorithm is currently not tested quantitatively, it produces qualitatively realistic retreat of the outer bank in meander bends, with enhanced erosion rates at tighter bends. Channel migration, however, requires not only lateral erosion along the outer bank, but also deposition along the inner bank. We applied two different algorithms to simulate deposition and the redistribution of sediment within the channel, both of which have flaws. The first approach fails to maintain the sediment mass balance and has little or no basis in the depositional processes that operate within river channels, yet produces visually appropriate results. The second, more successful method has a better grounding and implements a simple algorithm for lateral or cross-stream circulation patterns, which are thought to govern the deposition of material on point bars. Indeed, this method leads to the development of such features, which in itself is a significant step in the enhancement of cellular river models.

Additionally, we are only simulating the effects of curvature-induced secondary flow on lateral erosion. This implies, firstly, that because we are implementing erosion explicitly, without changing the model flow dynamics, we may only be recreating the symptoms of lateral erosion, not the causes. Secondly, like all curvature-driven lateral erosion models (e.g. the IPS models), our cellular automaton model requires the existence of an initial curvature in the channel for the effective simulation of meander development. However, as our model is cellular, the deposition of bed material due to the regular erosion/depositional processes within the channel may cause the thalweg to shift to one side, which would then trigger lateral erosion.

Due to these limitations, one might question whether we can use such cellular models to further our understanding of river meandering. In response, we argue that our model needs to be developed, and that the two methods of sediment redistribution are only used to illustrate the concept that meandering can be calculated within a CA framework

driven by the R_{ca} algorithm. At worst, even if we cannot use this method to learn about the causes of lateral erosion and meandering, we can use it to determine how meandering can influence valley floor and river catchment evolution.

Nonetheless, we have identified further areas for development.

1. The algorithm needs adaptation to address meander cut-offs.
2. The routine for sediment deposition along the inside bend needs to be improved. A possible approach might be the delineation of transport vectors using successive cross-stream gradients.
3. The model needs to be tested for sensitivity. The effects of internal factors, such as number of smoothing passes, as well as external factors, such as hydrograph variability, need to be examined. A particular question in this respect concerns the robustness of the edge detection method during overbank flood events.
4. Currently, the model mainly simulates meander extension. Additional changes to the model are required to simulate the downstream migration of meander bends.
5. The model needs to be calibrated and validated for both migration rates and planform sinuosities.

Conclusions

These preliminary simulations demonstrate the successful calculation and integration of regional curvature parameters within a CA model to drive lateral erosion. As CAESAR has been used previously to simulate braided river dynamics (Hicks *et al*., 2004) we firmly believe that both processes can be modelled in the same simulation. As such, we believe this is a significant step towards the development of generic fluvial landscape evolution models, that could further the theoretical understanding of fluvial systems.

Acknowledgements

M.J.V. was funded by NERC grant NER/A/S/2001/00454. The CAESAR model used in this paper can be downloaded at no charge from http://www.coulthard.org.uk

References

Blondeaux P, Seminara G. 1985. A unified bar-bend theory of river meanders. *Journal of Fluid Mechanics* **157**: 449–470.

Coulthard TJ Macklin MG. 2003. Modeling long-term contamination in river systems from historical metal mining. *Geology* **31**(5): 451–454.

Coulthard TJ, Kirkby MJ, Macklin MG. 2000. Modelling geomorphic response to environmental change in an upland catchment. *Hydrological Processes* **14**: 2031–2045.

Coulthard TJ, Macklin MG, Kirkby MJ. 2002. A cellular model of Holocene upland river basin and alluvial fan evolution. *Earth Surface Processes and Landforms* **27**: 269–288.

Ferguson RI. 1976. Disturbed periodic model for river meanders. *Earth Surface Processes* **1**: 337–347.

Hasegawa K. 1989. Universal bank erosion coefficient for meandering rivers. *Journal of Hydraulic Engineering, ASCE* **115**(4): 744–765.

Hicks DM, Walsh J, Coulthard TJ. 2004. Effects of changing flow regime, sediment supply, and riparian vegetation on the morphology of the braided Waitaki river, New Zealand. *Eos Transactions AGU* **85**(47): Abstract H42B-01.

Howard AD. 1992. Modelling channel migration and floodplain sedimentation in meandering streams. In *Lowland Floodplain Rivers: Geomorphological Perspectives*, Carling PA, Petts GE (eds). John Wiley: Chichester: 1–41.

Howard AD. 1996. Modelling channel evolution and floodplain morphology. In *Floodplain Processes*, Anderson MG, Walling DE, Bates PD (eds). John Wiley: Chichester; 15–62.

Howard AD, Knutson TR. 1984. Sufficient conditions for river meandering: A simulation approach. *Water Resources Research* **20**(11): 1659–1667.

Ikeda S, Parker G, Sawai K. 1981. Bend theory of river meanders: I. Linear development. *Journal of Fluid Mechanics* **112**: 363–377.

Johanneson H, Parker G. 1989. A linear theory of meanders. In *River Meandering*, Ikeda S, Parker G (eds). Water Resources Monograph. American Geophysical Union: Washington, DC: 181–213.

Lancaster ST, Bras RL. 2002. A simple model of river meandering and its comparison to natural channels. *Hydrological Processes* **16**: 1–26.

Lauer JW, Parker G. 2005. Net transfer of sediment from floodplain to channel on three southern US rivers. Proceedings, ASCE World Water and Environmental Resources 2005 Congress, Anchorage; 1–12.

Murray AB, Paola C. 1994. A cellular model of braided rivers. *Nature* **371**: 54–57.

Paola C. 2000. Modelling stream braiding over a range of scales. In *Gravel Bed Rivers 5*. Hydrological Society Inc.: Wellington, New Zealand; 11–38.

Sun T, Meakin P, Jøssang T, Schwarz K. 1996. A simulation model for meandering rivers. *Water Resources Research* **32**(9): 2937–2954.
Sun T, Meakin P, Jøssang T. 2001a. A computer model for meandering rivers with multiple bedload sediment sizes. 1. Theory. *Water Resources Research* **37**(8): 2227–2241.
Sun T, Meakin P, Jøssang T. 2001b. A computer model for meandering rivers with multiple bedload sediment sizes. 2. Computer simulations. *Water Resources Research* **37**(8): 2243–2258.
Thomas R, Nicholas AP. 2002. Simulation of braided flow using a new cellular routing scheme. *Geomorphology* **43**: 179–195.

